Als2-deficient mice exhibit disturbances in endosome trafficking associated with motor behavioral abnormalities

R. S. Devon*†‡, P. C. Orban*†, K. Gerrow§, M. A. Barbieri¶, C. Schwab*, L. P. Cao*, J. R. Helm*, N. Bissada*, R. Cruz-Aguado*, T.-L. Davidson*, J. Witmer*, M. Metzler*, C. K. Lam‖, W. Tetzlaff‖, E. M. Simpson*, J. M. McCaffery**, A. E. El-Husseini§, B. R. Leavitt*, and M. R. Hayden*††

*Centre for Molecular Medicine and Therapeutics, Department of Medical Genetics, University of British Columbia, and Child & Family Research Institute, 980 West 28th Avenue, Vancouver, BC, Canada V5Z 4H4; §Department of Psychiatry, Brain Research Centre, University of British Columbia, Vancouver, BC, Canada V6T 2A1; ¶Department of Biological Sciences, Florida International University, Miami, FL 33199; **Integrated Imaging Center, Department of Biology, The Johns Hopkins University, Baltimore, MD 21218; and ‖International Collaboration on Repair Discoveries and Department of Zoology, University of British Columbia, Vancouver, BC, Canada V6T 1Z4

Edited by Huda Y. Zoghbi, Baylor College of Medicine, Houston, TX, and approved April 27, 2006 (received for review November 24, 2005)

ALS2 is an autosomal recessive form of spastic paraparesis (motor neuron disease) with juvenile onset and slow progression caused by loss of function of alsin, an activator of Rac1 and Rab5 small GTPases. To establish an animal model of ALS2 and derive insights into the pathogenesis of this illness, we have generated alsin-null mice. Cytosol from brains of *Als2*$^{-/-}$ mice shows marked diminution of Rab5-dependent endosome fusion activity. Furthermore, primary neurons from *Als2*$^{-/-}$ mice show a disturbance in endosomal transport of insulin-like growth factor 1 (IGF1) and BDNF receptors, whereas neuronal viability and endocytosis of transferrin and dextran seem unaltered. There is a significant decrease in the size of cortical motor neurons, and *Als2*$^{-/-}$ mice are mildly hypoactive. Altered trophic receptor trafficking in neurons of *Als2*$^{-/-}$ mice may underlie the histopathological and behavioral changes observed and the pathogenesis of ALS2.

ALS | alsin | knockout mouse | motor neuron | Rab5

Mutations in the *ALS2* gene cause autosomal recessive juvenile onset amyotrophic lateral sclerosis (ALS2) and the related conditions infantile onset ascending hereditary spastic paraplegia (IAHSP) and juvenile onset primary lateral sclerosis (JPLS) (1–5). IAHSP and JPLS are characterized by degeneration of upper motor neurons of the corticospinal and spinocerebellar tracts, whereas a diagnosis of ALS also requires lower motor neuron involvement. The expression pattern of *Als2* is consistent with this pattern of neurodegeneration, because the gene is expressed primarily in neurons of the CNS, including cortical motor neurons and the large alpha motor neurons of the spinal cord. Interestingly, however, it is also found at particularly high levels in the granule cell neurons of the cerebellum, a region not previously implicated in ALS (6).

Alsin, the protein encoded by *ALS2*, has been characterized as a novel guanine nucleotide exchange factor (GEF) for Rab5 and Rac1 (7–9). Rab5 is known to be an important factor in many stages of endocytosis and the early trafficking of signaling molecules (10–13). In neurons, Rab5-mediated endocytic trafficking is essential for presynaptic transmission at the *Drosophila* neuromuscular junction (14), and Rab5 is required for the formation of endocytic pits for internalization of α-amino-3-hydroxy-5-methyl-4-isoxazolepropionic acid (AMPA) receptors after the induction of long-term depression (LTD) (15).

To reconcile the divergent activities of Rab5, it has been proposed that Rab5 is compartmentalized and activated for specific functions through interaction with particular GEFs and effector proteins (16). Its interaction with alsin has been suggested to modulate the signaling of neurotrophic factors (7).

All described mutations in the *ALS2* gene are predicted to cause premature protein termination and loss of function of the alsin protein (5). Therefore, we sought to investigate the effect of alsin deficiency in mice, to further understand human ALS2, and with regard to the role of alsin in the trafficking of specific neurotrophic receptors.

Results

***Als2*$^{-/-}$ Mice Are Viable and Fertile.** *Als2*-deficient mice were generated by using promoter trap gene targeting in ES cells to replace exons 3 and 4 of the *Als2* gene with an SA-IRES-βgeo-pA [splice acceptor-internal ribosome entry site-β-galactosidase-neomycin–poly(A) addition site] cassette encoding a bifunctional lacZ–neomycin fusion protein (17). The resulting protein encoded from the *Als2* locus would comprise only the five N-terminal amino acids of alsin fused to lacZ-neomycin, thereby inactivating both the full-length and the proposed short form of alsin (1, 2). Five homologous recombinant ES cell clones were confirmed to be correctly targeted, of which two were used to generate mouse lines for analysis (Fig. 1 *A* and *B*). Absence of alsin in *Als2*$^{-/-}$ mice was confirmed by Western blotting (Fig. 1*C*). The genotypes of progeny of heterozygous intercrosses showed a normal Mendelian distribution (genotypes from line 1: *Als2*$^{+/+}$, $n = 124$ (22.9%); *Als2*$^{+/-}$, $n = 278$ (51.3%); *Als2*$^{-/-}$, $n = 140$ (24.8%)). *Als2*$^{-/-}$ mice were indistinguishable from their WT littermates in size, appearance, and observed behavior in the home cage. Comparison of the number of progeny from homozygous *Als2*$^{-/-}$ mating pairs versus WT mating pairs over an 8-month period indicated that alsin deficiency did not affect fertility or fecundity (data not shown).

The Nervous System of *Als2*$^{-/-}$ Mice Exhibits Significant but Subtle Neuropathological Changes. Because ALS in humans is characterized by neurodegeneration in the brain and spinal cord, we assessed *Als2*$^{-/-}$ mice histologically for evidence of this. We performed TUNEL (Roche, Indianapolis), Fluorojade-B (Chemicon, Temecula, CA) staining, and immunostaining for cleaved caspase-3 of brain sections of WT and *Als2*$^{-/-}$ mice at

Conflict of interest statement: No conflicts declared.

This paper was submitted directly (Track II) to the PNAS office.

Abbreviations: ALS2, autosomal recessive juvenile onset ALS; GEF, guanine nucleotide exchange factor; CGN, cerebellar granule cell neuron; IGF1, insulin-like growth factor 1; IGF1R, IGF1 receptor; EEA1, early endosome antigen 1.

†R.S.D. and P.C.O. contributed equally to this work.

‡Present Address: Medical Genetics Section, University of Edinburgh Molecular Medicine Centre, Western General Hospital, Crewe Road, Edinburgh EH4 2XU, United Kingdom.

††To whom correspondence should be addressed. E-mail: mrh@cmmt.ubc.ca.

GENETICS

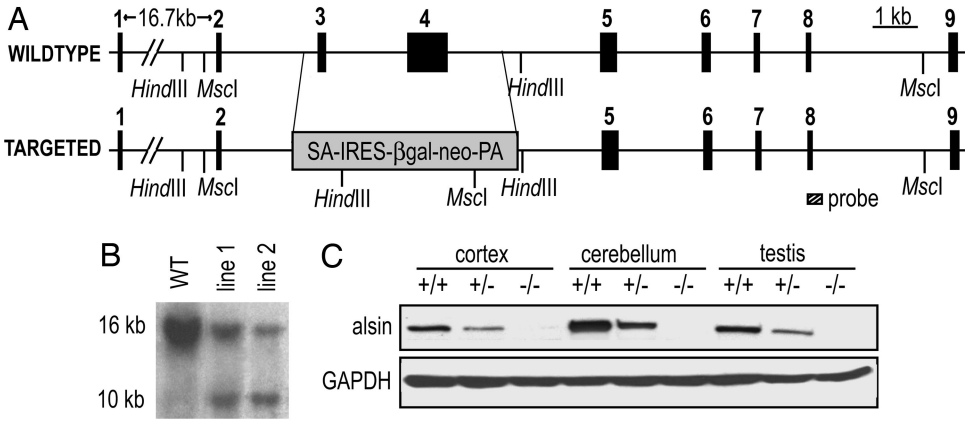

Fig. 1. Generation of *Als2*$^{-/-}$ mice. (*A*) The 5′ end of the WT *Als2* locus and the targeted allele, in which exons 3 and 4 were replaced. The Southern blotting probe is shown as a hatched box. (*B*) Southern blot of MscI-digested WT ES cell DNA (WT) and two targeted ES cell clones (lines 1 and 2). WT (16 kb) and targeted (10 kb) alleles are present as expected. (*C*) Western blot analysis of cortex, cerebellum, and testis from WT (+/+), *Als2*-heterozygous (+/−), and *Als2*-null (−/−) mice showing absence of alsin in homozygous targeted mice and reduced expression in heterozygotes.

3, 6, and 12 months. We did not find any evidence of increased apoptosis or necrosis.

To assess other possible neuropathological changes in these mice, we performed unbiased stereological assessments of brain, spinal cord, and sciatic nerve at 12 and 22 months of age. At 12 months, cell bodies of pyramidal motor neurons in layer V of the motor cortex of *Als2*$^{-/-}$ mice were significantly smaller than those of their WT counterparts (7% reduction in mean cell area; $P = 0.006$; Table 1, which is published as supporting information on the PNAS web site). All other measures of neuronal size revealed that neurons of *Als2*$^{-/-}$ mice had smaller cell bodies and axons of diminished caliber compared with WT, but no other measurement reached statistical significance (Table 1). The trend toward reduced size in *Als2*$^{-/-}$ mice was also apparent for cerebellar weight and total brain weight (Table 1). No further decrease in cortical neuron size was found in mice aged 22 months.

Conventional thin section electron microscopy analysis was carried out on brain and spinal cord of WT and *Als2*$^{-/-}$ mice. For the brain, coronal sections containing regions of the cerebrum, hippocampus, cerebellum, and brainstem were analyzed, whereas transverse sections from both the thoracic and lumbar spinal cord were examined. In each case, no discernible difference in ultrastructure was observed between WT and *Als2*$^{-/-}$ mice (data not shown).

To assess whether neuropathology typically found in human ALS and mutant superoxide dismutase 1 (SOD1) transgenic mice (18) was present in aged *Als2*$^{-/-}$ mice, we stained motor cortex, spinal cord, and cerebellum sections of 22-month-old animals with antibodies against ubiquitin, phosphorylated neurofilament (SMI31) and glial markers [glial fibrillary acidic protein (GFAP) for astroglia and Iba1 for microglia]. In addition, we stained with NeuN, calbindin antibodies, and cresyl violet to evaluate cellular architecture. No differences were seen, and no inclusions or abnormal neuronal processes (axonal spheroids, swellings) were found in sections stained with ubiquitin or SMI31. No astroglial or microglial activation could be demonstrated in cortex, hippocampus, or cerebellum, nor did we see evidence of glial activation in motor neuron areas or fiber tracts of the spinal cord.

Cytosol from Brains of *Als2*$^{-/-}$ Mice Exhibits Reduced Rab5-Dependent Fusion of Early Endosomes. It is well established that alsin interacts with and activates Rab5 (7–9). To assess early endosome fusion activity [known to be Rab5-dependent (12)], we used an *in vitro* assay of fusion activity, in which cytosolic test extracts are added to suitably labeled early endosomes, and the degree of resultant fusion assessed by colorimetry (19). Addition of cytosol from *Als2*$^{-/-}$ mouse brain resulted in up to 72% less fusion activity than cytosol from WT mouse brain (Fig. 2). WT brain cytosol supported endosome fusion in a concentration-dependent manner (Fig. 2*A*).

Exogenous alsin rescued the deficit in *Als2*$^{-/-}$ mouse brain cytosol. Lysate from SF9 cells expressing alsin using a baculovirus vector (7), but not control or heat-inactivated SF9 lysate,

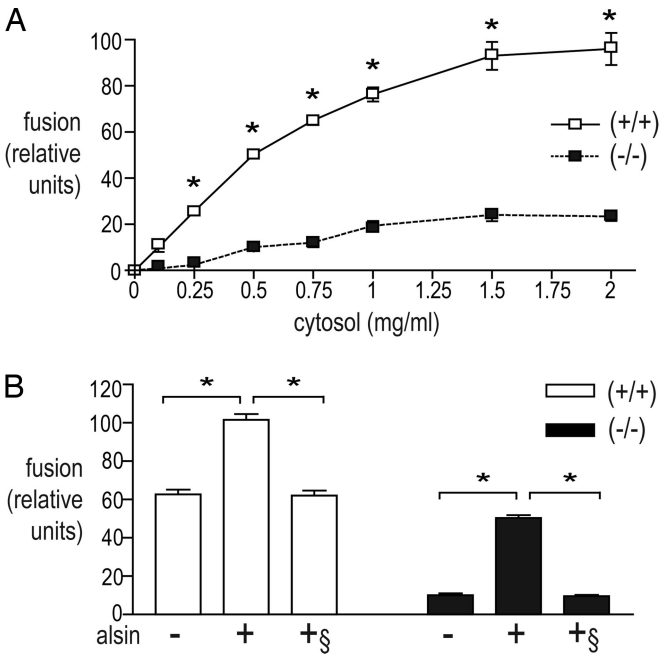

Fig. 2. Brain cytosol of *Als2*$^{-/-}$ mice is deficient in early endosome fusion activity. (*A*) Fusion activity of indicated concentrations of WT (open squares) or *Als2*$^{-/-}$ (filled squares) brain cytosol (means ± SD of triplicates). Fusion activity was significantly different (*, $P < 0.001$) between *Als2*$^{-/-}$ and WT. (*B*) Exogenous alsin restores the endosomal fusion activity in cytosol from *Als2*$^{-/-}$ brains. Brain cytosol (0.75 mg/ml) was supplemented with lysates of SF9 cells that had been transfected with vector alone (−), vector-expressing alsin (+), or heat-inactivated SF9 alsin^{+} lysate (+§) (means ± SD from three experiments). Addition of exogenous alsin resulted in a significant increase in fusion activity for WT (open bars) and *Als2*$^{-/-}$ (filled bars) mice (*, $P < 0.001$); this effect was abolished if heat-inactivated alsin^{+} lysate was used (*, $P < 0.001$).

restored endosome fusion activity ($P < 0.001$) (Fig. 2*B*). Interestingly, the addition of alsin also enhanced the endosome fusion activity of WT brain cytosol (Fig. 2*B*).

Neurons from *Als2*$^{-/-}$ Mice Exhibit Disturbances of Receptor Trafficking. We postulated that an impediment in endosomal trafficking of neurotrophin receptors, and resultant diminution in neurotrophic support, might be responsible for the reduction in neuronal size in *Als2*$^{-/-}$ mice. We analyzed cortical neurons and cerebellar granule cell neurons (CGNs) in culture, because both these cell types express alsin at high levels (6) and cortical neurons in particular are affected in ALS.

Neuronal morphology and survival in WT and *Als2*$^{-/-}$ neuron cultures were examined by DiI staining, fluorescence, and differential interference contrast (DIC) microscopy. No differences in morphology, size, or survival were noted between WT and *Als2*$^{-/-}$ neurons, and survival was between 85% and 95% for both genotypes (data not shown). There was also no difference between WT and *Als2*$^{-/-}$ CGNs in response to induction of apoptosis using low potassium culture conditions (5 mM as opposed to 25 mM), as assessed by a substrate-based assay for caspase 3 activity, immunoblotting of active caspase 3, or TUNEL staining (data not shown).

We initially examined whether a reduction in Rab5-GEF activity caused by the absence of alsin may result in abnormal trafficking of neurotrophic factor receptors. After 3 h of trophic factor deprivation, cortical or CGNs at 8–12 days in culture were treated by bath application of 50 ng/ml BDNF for between 5 and 180 min, and the positions of the BDNF receptor, TrkB, were assessed by indirect immunofluorescence. In both cell types, there was a marked difference between WT and *Als2*$^{-/-}$ neurons in the accumulation of fluorescence in the cell bodies (Fig. 3*A*, from cortical neurons). WT but not *Als2*$^{-/-}$ neurons showed a significant increase in perinuclear anti-TrkB staining in the first 60 min of BDNF stimulation (Fig. 3*B*).

There was no general disturbance of endocytosis, because uptake of Alexa Fluor 549-conjugated transferrin (Fig. 3 *C* and *D*) or FITC-conjugated dextran (not shown) showed no difference between WT and *Als2*$^{-/-}$ cultures.

We next repeated the BDNF stimulation experiment using insulin-like growth factor 1 (IGF1) and antibody to its receptor, IGF1R. After 30 min or more of IGF1 stimulation, puncta of at least 3.5 μm^2 area (calculated after flattening the confocal images) were apparent in the dendrites of some (between 1/200 and 1/2,000) *Als2*$^{-/-}$ CGNs (Fig. 4*A*). All positive cells contained at least 20 large puncta throughout several dendrites. *Als2*$^{-/-}$ cells were, on average, 1,000 times more likely to display this phenotype than WT cells (four separate cultures examined at the 60-min stimulation time point). To define the nature of the IGF1R puncta, the cells were costained with markers of endocytic compartments. As shown in Fig. 4 *C* and *D*, 32% of the puncta colocalized with early endosome antigen 1 (EEA1), and the majority (86%) colocalized with Rab5, both markers of early endosomes, and 17% colocalized with Rab11, a marker of recycling endosomes (Fig. 4*E*). Similar results were obtained with cortical neurons, but a smaller proportion of the *Als2*$^{-/-}$ cells showed the phenotype.

There was no significant change in the total amount of IGF1 or BDNF receptor present during the course of the stimulation, nor was there any apparent difference between the amount of receptor present in WT and *Als2*$^{-/-}$ neurons in culture (Fig. 6, which is published as supporting information on the PNAS web site). Control experiments confirming that these results were not due to receptor synthesis during the experiment and that the changes were stimulus-specific are described in *Supporting Materials and Methods* (*Receptor Trafficking Controls*), which is published as supporting information on the PNAS web site. In a sciatic nerve crush (ligation) experiment to assess motor

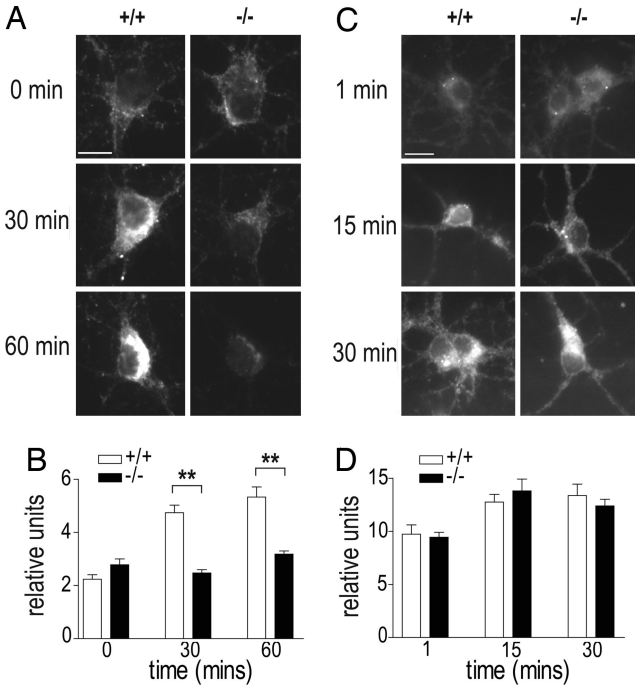

Fig. 3. Neurons from *Als2*$^{-/-}$ mice show disturbances of BDNF receptor (TrkB) endocytosis. (*A*) *Als2*$^{-/-}$ cortical neurons show markedly less increase in fluorescence in the cell-body region after stimulation with BDNF than WT neurons. (*B*) Cell-body region TrkB fluorescence after BDNF stimulation, quantified in cortical neurons randomly selected by using differential interference contrast (DIC) microscopy (**, $P < 0.01$; 14–20 cells for each time point and genotype). (*C*) There is no difference in transferrin uptake between WT and *Als2*$^{-/-}$ neurons: after 30 min, both show intense transferrin fluorescence in their cell bodies. (*D*) Cell-body region fluorescence in a representative transferrin uptake time course, quantified in neurons randomly selected by using DIC microscopy. (Scale bars: 10 μm.)

neuron transport *in vivo*, IGF1R-positive puncta were visible in motor axons of *Als2*$^{-/-}$ but not WT mice (Fig. 7, which is published as supporting information on the PNAS web site), consistent with endosome trafficking defects. However, we found no genotype-linked difference in rapid axonal transport (as evidenced by 8 h accumulation at a ligature) of IGF1R, TrkB, or choline acetyl transferase (ChAT) (three WT and three *Als2*$^{-/-}$ 22-month-old mice).

To identify intracellular signaling changes that might accompany the apparent trafficking disturbances, we stimulated starved neurons with IGF1 or BDNF and assessed phosphorylation of Akt and extracellular signal-regulated kinases (ERKs). Although primary fibroblasts from *Als2*$^{-/-}$ mice did show a significant decrease in Akt phosphorylation after stimulation with IGF1 ($n = 2$, $P = 0.033$), we did not find any significant differences in these indices of signal transduction between WT and *Als2*$^{-/-}$ neurons (Fig. 8, which is published as supporting information on the PNAS web site).

Western blot analyses showed no apparent differences in the abundance of 13 intracellular trafficking pathway components, including other Rab GTPases and synaptic vesicle proteins, in cerebral cortical extracts and cerebellar extracts of 18-month-old WT and *Als2*$^{-/-}$ mice (Fig. 9, which is published as supporting information on the PNAS web site).

***Als2*$^{-/-}$ Mice Are Hypoactive.** A cohort of 40 mice (20 each WT and *Als2*$^{-/-}$) was followed until 15 months of age for assessment of activity and motor skills. During this time, four WT and one *Als2*$^{-/-}$ mouse died or had to be euthanized. These observations

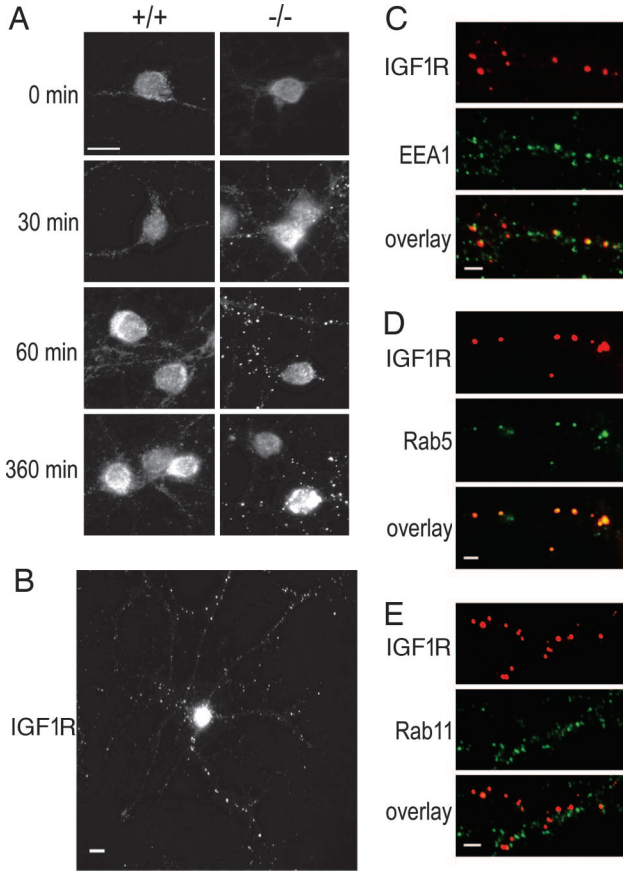

Fig. 4. Neurons from *Als2*$^{-/-}$ mice show disturbances of IGF1R endocytosis. (*A*) CGNs were stimulated with IGF1 for 0, 30, 60, and 360 min before staining with antibodies to the IGF1R alpha chain. Note the large puncta seen at later time points in *Als2*$^{-/-}$ neurons. (*B*) A cell with puncta is shown at lower magnification. (*C–E*) *Als2*$^{-/-}$ neurons, as in *A*, but stained with both anti-IGF1R and antibodies to EEA1 (*C*), Rab5 (*D*), or Rab11 (*E*). A large majority of IGF1R-positive puncta costain with anti-Rab5, a smaller proportion with anti-EEA1, and few with anti-Rab11. (Scale bars: 10 μm.)

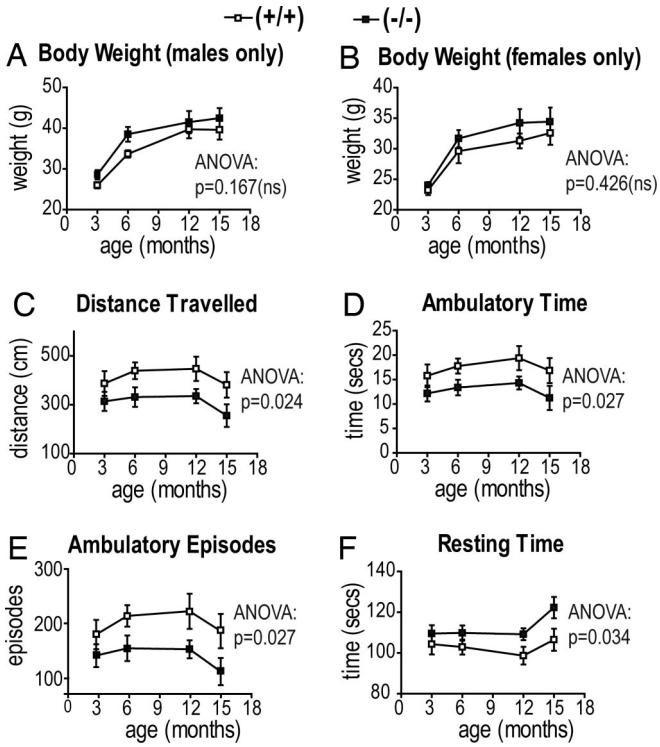

Fig. 5. *Als2*$^{-/-}$ mice show a tendency to increased body weight and are hypoactive. Body weight for male (*A*) and female (*B*) *Als2*$^{-/-}$ mice (filled squares) shows a trend but no significantly increased weight gain compared with WT littermates (open squares). (*C–F*) Exploratory open-field activity for *Als2*$^{-/-}$ mice (filled squares) versus WT mice (open squares) shows that *Als2*-null mice are hypoactive throughout their life (two-way ANOVA, $P < 0.05$ for each measure). Values shown are means ± SEM of $n = 19–20$ mice ($n = 9–10$ each males and females).

indicate that absence of alsin does not adversely affect lifespan, at least until 15 months of age. Measurements of body weight revealed no difference between male or female *Als2*$^{-/-}$ and WT mice, although there was a trend toward increased body weight, particularly for male *Als2*$^{-/-}$ mice (two-way ANOVA, $P = 0.167$ for males and $P = 0.426$ for females) (Fig. 5 *A* and *B*).

In a 3-min open-field trial to measure exploratory activity, *Als2*$^{-/-}$ homozygotes were significantly hypoactive compared with WT mice. Two-way repeated-measures ANOVA revealed a significant effect of genotype across the time course of the experiment in measures of distance traveled ($P = 0.024$, Fig. 5*C*), time ambulating ($P = 0.027$, Fig. 5*D*), number of ambulatory episodes ($P = 0.027$, Fig. 5*E*), and time resting ($P = 0.034$, Fig. 5*F*). This phenotype was evident in even the youngest mice (3 months of age) and showed little if any worsening over time.

Apart from hypoactivity, *Als2*$^{-/-}$ mice showed no other deficits in motor skills and coordination. Grip strength and latency to fall from an accelerating rotarod were both indistinguishable from WT. *Als2*$^{-/-}$ mice did not show evidence of deficit in the leg extension reflex (hind-limb "clasping"), when suspended by the tail. Additionally, there was no difference between WT and *Als2*$^{-/-}$ mice in the proportion of time spent in the perimeter versus central areas of the arena.

Discussion

The absence of alsin in mice results in a pronounced cellular phenotype, and subtle neuropathology and behavioral changes that are consistent with motor neuron disease. Brain cytosol from *Als2*$^{-/-}$ mice showed a marked decrease in ability to support Rab5-dependent endosome fusion *in vitro*. Furthermore, cultured neurons from *Als2*$^{-/-}$ mice showed abnormalities in the endosomal transport of receptors for the neurotrophic factors BDNF and IGF1. *Als2*$^{-/-}$ mice exhibit a decrease in locomotor activity and a small but significant decrease in the size of cortical motor neurons.

Because alsin has previously been shown to be a Rab5-GEF (7, 8), we focused on examining cellular phenotypes related to Rab5 activity, namely, early endosome trafficking and fusion. We observed dramatic reduction in Rab5-dependent endosome fusion activity in *Als2*-null brain cytosol. This finding suggests that alsin is an important component of early endosome fusion activity in adult mouse brain.

An abnormal accumulation of large, IGF1R-positive puncta was seen in *Als2*$^{-/-}$ neurons after IGF1 stimulation and in sciatic nerve motor axons. The puncta in cultured neurons primarily colocalized with markers of early endosomes (Rab5 and EEA1), suggesting that they represent aberrant early endosome components of the IGF1R endocytosis pathway, reflecting a failure of normal maturation of these endosomes. This finding may imply a role for alsin in conversion from early to late endosomes, a process that has been shown to require the activity of a Rab7 GEF, the class C VPS/HOPS complex (20). Interestingly, IGF1 has long been flagged as a potential therapeutic agent for ALS because of its ability to promote motor neuron survival. Recently, it has been shown to confer a modest benefit in human adult onset ALS (21) and to delay disease onset and ameliorate

progression in mutant superoxide dismutase 1 (SOD1) transgenic mice (21, 22).

Neurons from *Als2*-null mice also exhibited a defect in trafficking of TrkB when stimulated with its ligand, BDNF, whereas other forms of receptor-mediated and fluid-phase endosomal trafficking were unaffected. It is likely that aberrant growth factor receptor endocytosis in *Als2*-null mice results in a deficiency in trophic factor support of neurons lacking alsin. This trophic support is thought to be dependent on the transport of endosomes bearing activated receptors from the neurite to nucleus, resulting in transcriptional changes (23, 24). In experiments in which we assessed phosphorylation of Akt and extracellular signal-regulated kinases (ERKs), prominent components of the intracellular signaling pathways of IGF1 and BDNF, we found significant differences between WT and *Als2*-null fibroblasts but not neurons. It is possible that these assays are too crude to reveal subtle signaling defects in neurons or that alsin-null neurons have undergone compensatory changes in the regulation of signal transduction.

Als2-null mice exhibited subtle pathological changes in the CNS. At 12 months of age, cortical motor neurons of $Als2^{-/-}$ mice were slightly smaller than their WT counterparts, and there was a trend toward reduction in neuronal size and axonal caliber in all cell types observed. That this trend extends to lower motor neurons is consistent with the observation that *ALS2* mutation in humans can result in lower motor neuron symptoms. Neuronal shrinkage is strongly associated with motor neuron disease, particularly primary lateral sclerosis (PLS) (25). Additionally, in ALS, the largest alpha motor neurons are the most vulnerable to degeneration, although the role of axonal caliber in the etiology of motor neuron disease is as yet unclear (26). Because there have as yet been no published descriptions of pathological investigations in ALS2 patients, the precise expected findings in mice are not obvious.

In the context of ALS pathogenesis, it is interesting to note that it is only the cortical motor neurons of $Als2^{-/-}$ mice that exhibit both functional and histopathological abnormalities, even though CGNs express the highest levels of alsin in the mouse brain (6). The abnormal IGF1R puncta were seen less frequently in cortical neuron cultures than in CGNs, but this result is likely to reflect the fact that sensory neurons within cortical cultures do not express alsin. The selectivity toward motor neuron pathology may be due to the larger size of motor neurons, or peculiarities of calcium homeostasis, which may make them particularly vulnerable to decreases in trophic support (reviewed in ref. 27).

In humans, *ALS2*-related disease causes severe spastic paraparesis with onset in childhood and slow progression, and its autosomal recessive pattern of inheritance suggests complete loss of alsin function. The early onset of hypoactivity in *Als2*-null mice and the fact that it did not worsen over time are consistent with this finding. Nevertheless, a more obvious phenotype in $Als2^{-/-}$ mice might have been predicted. This incongruity is unlikely to be due to simple redundancy of protein function, because there is no other protein in the mouse (or human) that shares the same complement of domains as alsin. The closest related protein, ALS2 C-terminal-like (ALS2CL) lacks alsin's N-terminal regulator of chromatin condensation (RCC1) domain, and is poorly expressed in the brain (6, 28). We have not found significant differences in the expression of ALS2CL between WT and $Als2^{-/-}$ motor cortex or cerebellum by quantitative RT-PCR (data not shown). We have also found no difference between WT and $Als2^{-/-}$ motor cortex or cerebellum in the abundance of 13 different neuronal trafficking-associated proteins. The absence of a dramatic phenotype may instead result from compensation by multiple Rab and Rac GEFs, whose activity, rather than mere abundance, may be altered. Alternatively, it may be related to the physical length of neurons in mouse versus human, whereby human motor neurons would have a much lower tolerance of defects in neurotrophic factor signaling and transport.

Our findings are in partial agreement with two recent descriptions of *Als2*-null mice (29, 30). All studies agree that $Als2^{-/-}$ mice exhibit no gross phenotype other than increased (or a trend toward increased) body weight. All three studies also demonstrate some impairment in motor function: early-onset hypoactivity (this study), or a significant, or trend toward, late-onset rotarod deficit (refs. 29 and 30, respectively). Histologically, Cai *et al*. (29) demonstrated no abnormalities, whereas Hadano *et al*. (30) showed astrocytosis and activation of microglia and a late-onset loss of Purkinje cells and lower motor neuron axons. The reason for these discrepancies is unclear; however, they are possibly due to differences in the ES cells used, leading to differences in the background strain of experimental mice, or to differences in design of the targeting vectors. In culture, Hadano *et al*. (30) showed subtle defects in early trafficking of EGF in *Als2*-deficient fibroblasts, whereas Cai *et al*. (29) demonstrated increased susceptibility to oxidative stress in cortical neurons. Our description of defects in early endosomal trafficking and fusion in *Als2*-null mice may provide a mechanism for the increased susceptibility to oxidative stress seen (29). The Rab5-associated endocytic activity of cells has been shown to increase in response to oxidative stress via the mitogen-activated protein kinase (MAPK) p38 (31). Cells lacking alsin may be more vulnerable to oxidative stress than WT cells, as a direct result of their defect in this adaptive Rab5-associated endocytic response.

In conclusion, we have demonstrated that *Als2*-deficient mice have subtle motor neuron pathology and motor behavior abnormalities and that neurons from these mice show marked defects in specific endosomal trafficking pathways with a severe deficit in early endosome fusion stimulating activity *in vitro*. These abnormalities are likely to be related to the role of alsin as a GEF for Rab5 and may provide a cellular mechanism associated with the pathogenesis of ALS2.

Materials and Methods

Further details are described in *Supporting Materials and Methods*.

***Als2* Gene Targeting.** A targeting construct was generated in the promoter trap vector pIFS (17) to replace *Als2* exons 3 and 4 with an SA-IRES-βgeo-PA [splice acceptor-internal ribosome entry site-β-galactosidase-neomycin–poly(A) addition site] cassette (Fig. 1*A*). The construct was electroporated into 2×10^7 mEMS128 ES cells. Five correctly targeted clones were confirmed by PCR and Southern blotting.

Generation of $Als2^{-/-}$ Mice. ES cells were microinjected into C57BL/6J blastocysts and implanted into pseudopregnant females to produce chimeras. Male chimeras from two clones were bred with C57BL/6J females, and F_1 $Als2^{+/-}$ heterozygotes were intercrossed to generate WT, heterozygous, and homozygous mice. The lines were maintained by backcrossing of heterozygotes with C57BL/6J mice. Absence of alsin in $Als2^{-/-}$ mice was confirmed by Western blotting using the N-alsin-24 monoclonal antibody (6) relative to a GAPDH control. All experiments were performed on two lines, with identical results, except for behavioral analysis, which was performed on line 1 only.

Histological Measurements. Tissues were prepared from 12- and 22-month-old WT and $Als2^{-/-}$ mice as described in Devon *et al*. (6). Motor neuron size and density were determined in 25-μm-thick cryostat sections. Measurements of cell size and axon diameter were performed in 5-μm-thick paraffin-embedded sections, or 500-nm semithin sections, respectively, stained with cresyl violet or toluidine blue and measured by using STEREOINVESTIGATOR software (Microbrightfield, Williston, VT). Data

were analyzed by using an independent-samples *t* test using SPSS software. For conventional electron microscopy, specimens were prepared as described (32). The grids were examined, and images were collected on a Philips (Eindhoven, The Netherlands) EM 410 transmission electron microscope (TEM) equipped with a Olympus Soft Imaging Solutions (Lakewood, CO) Megaview III digital camera.

***In Vitro* Endosome Fusion Assay.** Assessment of fusion of early endosomes loaded with either dinitrophenylated β-glucuronidase or mannosylated anti-dinitrophenyl IgG was performed as described (19). Results are presented as means and SDs and were analyzed by using an unpaired two-tailed Student's *t* test.

Preparation of Cytosol and Alsin Protein. Brain cytosol extracts from 3- to 4-month-old male and female *Als2*$^{-/-}$ and WT littermate mice were generated by homogenization of snap-frozen tissues followed by centrifugation to remove particulates. Alsin protein was supplied as supernatant of SF9 cells transfected with a baculovirus vector encoding full-length mouse alsin (7).

Neuronal Culture. Dissociated primary neuronal cultures were prepared from cerebellum of postnatal day 7–8 mice or cortex of day 16.5 embryos. IGF1 and BDNF stimulations were performed after starving cells for 3 h (in medium lacking serum for CGNs, or B27 supplement for cortical neurons). IGF1 or BDNF (50 ng/ml final concentrations) were added to the starvation medium and incubated for the indicated times before fixation.

Imaging and Analysis. Images were acquired on a Zeiss Axiovert M200 motorized microscope with a 63 × 1.4 NA ACROMAT oil immersion lens and a monochrome 14-bit Zeiss Axiocam HR charged-coupled camera with 1,300 × 1,030 pixels. Analysis was performed by using IMAGEJ (NIH) and NORTHERN ECLIPSE software (Empix Imaging, Mississauga, ON, Canada).

Behavioral Assessment. Forty F_2 mice (20 *Als2*$^{-/-}$ homozygotes and 20 WT littermate controls, each 10 females and 10 males) were tested. Locomotor activity was measured in an automated open-field apparatus (Medical Associates, St. Albans, VT). Forelimb grip strength was assessed by using a Chatillon Digital Force Gauge DFIS-2 (Columbus Instruments, Columbus, OH). Motor coordination and balance were assessed with an accelerating rotarod (0 to 45 rpm in 4 min). Comparisons were made by using unpaired two-tailed Student's *t* tests (95% confidence intervals) using PRISM 3.02 software (GraphPad, San Diego) and repeated measures two-way ANOVA using SPSS software.

Note Added in Proof. A recent paper (33) has described a JPLS patient with a missense mutation in *ALS2*.

We thank Dr. Andrew MacLeod for assistance with statistics, and Justin Topp, Sandy Severson, and Bruce Horazdovsky of the Mayo Foundation, who have generously shared their expertise and reagents with us. This work was supported by the Canadian Institutes for Health Research (separate grants to M.R.H., A.E.E.-H., W.T., and B.R.L.), the ALS Association (M.R.H.), the Spastic Paraplegia Foundation, Inc. (SPF) (M.R.H. and B.R.L.), the Jose Carreras International Leukemia Foundation (E. D. Thomas Program) at Florida International University (M.A.B.), the Canada Foundation for Innovation and the British Columbia Knowledge Development Fund (E.M.S.), the Canadian Genetic Disease Network (B.R.L.), the Michael Smith Foundation (A.E.E.-H.), and the EJLB Foundation (A.E.E.-H.). R.S.D. was the recipient of a Wellcome Trust International Prize Travelling Research Fellowship. E.M.S. holds a Canada Research Chair in Genetics and Behavior. A.E.E.-H. is a Canadian Institutes of Health Research new investigator and a Michael Smith Foundation for Health Research scholar. M.R.H. holds a Canada Research Chair in Human Genetics.

1. Hadano, S., Hand, C. K., Osuga, H., Yanagisawa, Y., Otomo, A., Devon, R. S., Miyamoto, N., Showguchi-Miyata, J., Okada, Y., Singaraja, R., *et al*. (2001) *Nat. Genet*. **29,** 166–173.
2. Yang, Y., Hentati, A., Deng, H. X., Dabbagh, O., Sasaki, T., Hirano, M., Hung, W. Y., Ouahchi, K., Yan, J., Azim, A. C., *et al*. (2001) *Nat. Genet*. **29,** 160–165.
3. Gros-Louis, F., Meijer, I. A., Hand, C. K., Dube, M. P., MacGregor, D. L., Seni, M. H., Devon, R. S., Hayden, M. R., Andermann, F., Andermann, E. & Rouleau, G. A. (2003) *Ann. Neurol*. **53,** 144–145.
4. Eymard-Pierre, E., Lesca, G., Dollet, S., Santorelli, F. M., di Capua, M., Bertini, E. & Boespflug-Tanguy, O. (2002) *Am. J. Hum. Genet*. **71,** 518–527.
5. Devon, R. S., Helm, J. R., Rouleau, G. A., Leitner, Y., Lerman-Sagie, T., Lev, D. & Hayden, M. R. (2003) *Clin. Genet*. **64,** 210–215.
6. Devon, R. S., Schwab, C., Topp, J. D., Orban, P. C., Yang, Y. Z., Pape, T. D., Helm, J. R., Davidson, T. L., Rogers, D. A., Gros-Louis, F., *et al*. (2005) *Neurobiol. Dis*. **18,** 243–257.
7. Topp, J. D., Gray, N. W., Gerard, R. D. & Horazdovsky, B. F. (2004) *J. Biol. Chem*. **279,** 24612–24623.
8. Otomo, A., Hadano, S., Okada, T., Mizumura, H., Kunita, R., Nishijima, H., Showguchi-Miyata, J., Yanagisawa, Y., Kohiki, E., Suga, E., *et al*. (2003) *Hum. Mol. Genet*. **12,** 1671–1687.
9. Kanekura, K., Hashimoto, Y., Kita, Y., Sasabe, J., Aiso, S., Nishimoto, I. & Matsuoka, M. (2005) *J. Biol. Chem*. **280,** 4532–4543.
10. McLauchlan, H., Newell, J., Morrice, N., Osborne, A., West, M. & Smythe, E. (1998) *Curr. Biol*. **8,** 34–45.
11. Sato, M., Sato, K., Fonarev, P., Huang, C. J., Liou, W. & Grant, B. D. (2005) *Nat. Cell Biol*. **7,** 559–569.
12. Gorvel, J. P., Chavrier, P., Zerial, M. & Gruenberg, J. (1991) *Cell* **64,** 915–925.
13. Nielsen, E., Severin, F., Backer, J. M., Hyman, A. A. & Zerial, M. (1999) *Nat. Cell Biol*. **1,** 376–382.
14. Wucherpfennig, T., Wilsch-Brauninger, M. & Gonzalez-Gaitan, M. (2003) *J. Cell Biol*. **161,** 609–624.
15. Brown, T. C., Tran, I. C., Backos, D. S. & Esteban, J. A. (2005) *Neuron* **45,** 81–94.
16. Zerial, M. & McBride, H. (2001) *Nat. Rev. Mol. Cell Biol*. **2,** 107–117.
17. Lefebvre, L., Viville, S., Barton, S. C., Ishino, F., Keverne, E. B. & Surani, M. A. (1998) *Nat. Genet*. **20,** 163–169.
18. Watanabe, M., Dykes-Hoberg, M., Culotta, V. C., Price, D. L., Wong, P. C. & Rothstein, J. D. (2001) *Neurobiol. Dis*. **8,** 933–941.
19. Barbieri, M. A., Li, G., Colombo, M. I. & Stahl, P. D. (1994) *J. Biol. Chem*. **269,** 18720–18722.
20. Rink, J., Ghigo, E., Kalaidzidis, Y. & Zerial, M. (2005) *Cell* **122,** 735–749.
21. Nagano, I., Ilieva, H., Shiote, M., Murakami, T., Yokoyama, M., Shoji, M. & Abe, K. (2005) *J. Neurol. Sci*. **235,** 61–68.
22. Kaspar, B. K., Llado, J., Sherkat, N., Rothstein, J. D. & Gage, F. H. (2003) *Science* **301,** 839–842.
23. Miaczynska, M., Pelkmans, L. & Zerial, M. (2004) *Curr. Opin. Cell Biol*. **16,** 400–406.
24. Howe, C. L. & Mobley, W. C. (2005) *Curr. Opin. Neurobiol*. **15,** 40–48.
25. Hudson, A. J., Kiernan, J. A., Munoz, D. G., Pringle, C. E., Brown, W. F. & Ebers, G. C. (1993) *Brain Res. Bull*. **30,** 359–364.
26. Nguyen, M. D., Lariviere, R. C. & Julien, J. P. (2000) *Proc. Natl. Acad. Sci. USA* **97,** 12306–12311.
27. von Lewinski, F. & Keller, B. U. (2005) *Neurosci. Lett*. **380,** 203–208.
28. Hadano, S., Otomo, A., Suzuki-Utsunomiya, K., Kunita, R., Yanagisawa, Y., Showguchi-Miyata, J., Mizumura, H. & Ikeda, J. E. (2004) *FEBS Lett*. **575,** 64–70.
29. Cai, H., Lin, X., Xie, C., Laird, F. M., Lai, C., Wen, H., Chiang, H. C., Shim, H., Farah, M. H., Hoke, A., *et al*. (2005) *J. Neurosci*. **25,** 7567–7574.
30. Hadano, S., Benn, S. C., Kakuta, S., Otomo, A., Sudo, K., Kunita, R., Suzuki-Utsunomiya, K., Mizumura, H., Shefner, J. M., Cox, G. A., *et al*. (2006) *Hum. Mol. Genet*. **15,** 233–250.
31. Cavalli, V., Vilbois, F., Corti, M., Marcote, M. J., Tamura, K., Karin, M., Arkinstall, S. & Gruenberg, J. (2001) *Mol. Cell* **7,** 421–432.
32. McCaffery, J. M. & Farquhar, M. G. (1995) *Methods Enzymol*. **257,** 259–279.
33. Panzeri, C., De Palma, C., Martinuzzi, A., Daga, A., De Polo, G., Bresolin, N., Miller, C. C., Tudor, E. L., Clementi, E. & Bassi, M. T. (May 2, 2006) *Brain*, 10.1093/brain/awl104.